'61

Distribution: limited
Provisional reproduction

UNESCO/NS/AZ/582
Rome Symposium, Paper no. 12

UNITED NATIONS EDUCATIONAL,
SCIENTIFIC AND CULTURAL ORGANIZATION

MAJOR PROJECT ON SCIENTIFIC RESEARCH ON ARID LANDS

Unesco/WMO symposium on changes of climate with special reference to the arid zones

Rome, 2 - 7 October 1961

A NUMERICAL STUDY OF THE EFFECT OF VERTICAL STABILITY ON MONSOONAL AND ZONAL CIRCULATIONS

by

E. B. Kraus, Woods Hole Oceanographic Institution

and

Edward N. Lorenz, Massachusetts Institute of Technology

ABSTRACT

About the turn of the century, rainfall volumes decreased rapidly along the equatorial and eastern margins of the arid zones as well as along the subtropical east coasts. This decrease seems to have been accompanied by an eastward shift in the mean position of the subtropical high pressure centers. From indirect observational evidence, it is concluded that the changes were associated with an increase of high-level westerly winds in lower middle latitudes. Qualitative theoretical considerations have suggested an association with changes in vertical stability.

The validity of this hypothesis is tested numerically. A two-layer model atmosphere is driven by a three-dimensional heating field, which is characterized by a meridional heating gradient, heating differences between a system of idealized oceans and continents, and a vertical heating gradient. The effect of variations in the vertical heating gradient upon the circulation is found to be compatible with observational deductions.

1. Introduction

The climatic pattern of the earth was perhaps never steady. Instrumental records can be used to document the most recent fluctuations. Their study has led one of us (Kraus 1960) to suggest that past surface climatic changes were probably associated with systematic changes of the mean vertical stability of the atmosphere, or--more precisely--of the mean vertical gradient of the cooling rate. A simplified numerical model has now been used in an initial attempt to test the dynamical aspects of this hypothesis. The model provides for an idealized system of warm continents and cool oceans, as well as latitudinal and vertical heating gradients. Variations of the latter have been found to produce in fact changes in the circulation regime which appear to be analogous to those observed in nature.

The analyses, both on the instrumental and on the numerical side, involve generalizations, simplifications and arbitrary selection of the numerical values for various model parameters. However, each step in the chain of reasoning is too complex for possible subconscious bias to have any predeterminable effect. The general agreement and compatibility of the results appears impressive in these circumstances, though they cannot be claimed to be conclusive at this stage.

2. Observed Recent Fluctuations of the Surface Climate

A striking feature of recent climatic variation was the abrupt decrease, about the turn of the century, of mean annual rainfall

volumes on the equatorial and eastern boundaries of the arid regions. The same happened along the subtropical east coasts. As evidence, the diagrams in figure 1. are reproduced here from an earlier paper. The change in low-latitude rainfall regimes was associated, in the temperate region of Australia, with an eastward shift of the climatic boundary between the mediterranean-type, winter-rainfall climate of South Australia and the east-coast type of climate which is characterized by more uniform rainfall with a tendency towards summer maxima.

While low latitude regions became drier, the climate tended to become warmer in many middle and high latitude regions of the northern hemisphere. This warming appears to have been more gradual or more irregular than the simultaneous change in the rainfall regime. It may have been associated again with an eastward shift of the climatic boundaries; in this case a tendency for a more maritime climate to spread eastward into the western temperate regions of the continents. There also is evidence for an increase in North Atlantic sea-surface temperatures at this time.

Instrumental and observational changes make the interpretation of surface pressure changes more dubious. Table 1 shows some evidence, though it is not convincing by itself, of an eastward shift in the mean position of the maritime subtropical anticyclone in the northern Atlantic at the beginning of this century. The pressure increase on the eastern stations is more than double the standard error.

Table 1. Mean annual station-level pressures (mb) in subtropical N. Atlantic

	Station	Period 1881-1900	Period 1901-1920	Difference
W. Atlantic	Bermuda	997.0	997.1	0.1
	Trinidad[1)]	996.4	996.6	0.2
E. Atlantic	Funchal	1016.3	1017.6	1.3
	Freetown	987.3	988.6	1.3

1) The height of the Trinidad barometer site was changed in 1900 from 133 ft. to 72 ft. This would imply a decrease in sea-level pressure there, unless an unpublished adjustment was made.

During the last 14 or 20 years a change in the opposite direction appears to have operated. There has been more rainfall in many low-latitude and east-coast regions and the warming trend seems to have been arrested temporarily. This has been associated with a distinct tendency for tropical hurricanes to reach the Australian or American east coasts, rather than take a more easterly course, as they appear to have done in the preceeding forty years.

3. The Association Between Upper Winds and Rainfall Regimes

A reasonably dense network of upper-air stations has become available only during the last ten or fifteen years. It is therefore not possible to interpret directly, from records, the climatic fluctuations of the last hundred years in terms of the three-dimensional circulation changes. However, it may be considered that the circulation patterns associated with a relatively cold and wet regime, or with a relatively warm and dry regime, should also predominate in individual years which exhibit these weather characteristics.

Table 2 lists rank correlation coefficients of mean zonal winds at 300 mb and seasonal rainfall in various parts of S.E. Australia.

Spearman's ranking correlation coefficient is

$$r_R = 1 - \frac{6 \Sigma d^2}{N^3 - N}$$

where Σd^2 is the sum of the squares of the differences between upper wind and rainfall ranks and N is the number of ranked seasons, viz. 14 winters and 12 summers in the present case. The approximate standard error of a rank correlation is

$$\sigma_R = (N - 1)^{-1/2}$$

Table 2. Ranking Correlation Coefficient of Mean Zonal Winds at 300 mb and of Rainfall in Southeastern Australia (1945-1959)

	Station	Ranking Correlation Coefficients Winter	Summer
Western plains	Wentworth	0.83	-0.78
	Euston	0.96	-0.94
	Balranald	0.90	-0.60
	Hay	0.88	-0.26
	Deniliquin	0.81	-0.89
	Yanko	0.83	-0.60
Eastern slopes and coast	Adaminaby	0.12	-0.89
	Cooma	-0.17	-0.66
	Bega	0.17	-0.83
	Kurrajong	-0.24	-0.94
	Sydney	-0.21	-0.71
Standard Error		0.28	0.30

The coefficients listed in Table 2 suggest a significant correlation between high westerlies and dry summers in the most easterly parts of Australia--a region affected by the general rainfall decrease at the turn of the century. Over the western plains, high upper winds are correlated significantly with increased winter rainfall and decreased summer rainfall. The resultant effect on annual rainfall is negligible, but high westerlies should be associated in this case with a more mediterranean climate with wetter winters and drier summers. This again corresponds to the observed change of the climate in that region at the beginning of the century. It is inferred that the high-level upper winds probably increased on the average at about that time.

A table similar to Table 2 was first derived by one of us (Kraus 1955) on the basis of a shorter data series (1945-1953). The ranking correlation coefficients were then found already to be considerably larger than their standard error. The additional indipendent data further increased the statistical significance of the deduced correlations and that is in itself of some relevance.

A strong negative correlation between upper winds and summer rainfall was shown in the earlier paper to exist also in tropical northeastern Australia. The similarity in the long-term rainfall time series along the subtropical east coasts of the United States and Australia suggests that a similar association may possibly be found there. No analysis has yet been made to find such a relation.

4. Stipulated Physical Causes

Any physical explanation of the recently observed climatic variations must be compatible with the observed pattern. This means that the time scale would have to be of the order of a half century or less. The process would have to be associated with a negative correlation between high-latitude surface temperatures and rainfall volumes along the subtropical east coasts and on the margin of the arid regions.

Most of the stipulated causes for climatic change appear to be incompatible with such an association. In particular, an increase in the solar constant, or an increase in the carbon dioxide mixing ratio, or a decrease in the turbidity or a primary warming of the ocean surface would all seem to cause higher surface temperatures to be associated with increased atmospheric instability, increased convection and therefore increased rainfall, and vice versa.

On the other hand, persistent variations of the ozone mixing ratio, in the lower stratosphere and in the upper troposphere, would tend to produce changes that have at least the right sign. An increased ozone amount would tend to produce higher surface temperatures in high latitudes and a lower tropopause with an increased overall static stability near the equator. This could also explain other features of the observed climatic change. In particular, it was thought (Kraus 1960) that storms of smaller dimensions would be suppressed in low latitudes, and that this could account for the reduction in the number of rainfall days, which had been observed to

be a characteristic feature of the general change at the beginning of this century. Disturbances of continental dimensions would be less affected, and this might explain the fact that in the typical monsoon regions the world-wide pattern of low-latitude rainfall change was least in evidence.

To test the validity of these deductions, we shall now try to relate them to a theoretical model. Our deductions will be supported if it is found that an externally imposed increase in the static stability is associated as expected: with decreased convection, supression of smaller storms, eastward shift of quasi-stationary pressure centers, and an increased zonal wind aloft.

5. The Equations of the Model

The climate of the world is affected by the internal dynamics of the atmosphere, and also by the influences of the sun and the underlying water and land surfaces. Likewise, the statistical properties (mean values, standard deviations, etc.) of an arbitrary system depend upon the internal dyanmics of the system, and also upon the statistical properties of the external influences. In those cases where the internal dynamics are expressible by a set of linear differential equations, an analytic deduction of the statistical properties of the system (output) from the statistical properties of the outside influences (input) is generally possible. When the governing dynamic equations are nonlinear, an analytic deduction of the output from the input is often difficult if not impossible, even though a definite relation between input and output exists.

In the case of the real atmosphere, the situation is further complicated by an incomplete knowledge of the dynamics.

With the advent of electronic computing machines, it has, however, become feasible to estimate the statistical properties of systems whose governing equations are known, by generating numerical solutions of the equations covering extended periods of time, and then collecting statistics from these solutions. Climatological values so obtained are not exact values, but are subject to sampling errors similar to those encountered in processing real data.

For the present study, we shall use the geostrophic form of the two-layer model derived by one of us (Lorenz, 1960 b). To the original form we append terms representing the nonadiabatic effects. A somewhat similar form of the equations was used by Bryan (1959).

The equations of the model can now be written in the following form:

$$\frac{\partial}{\partial t} \nabla^2 \psi = - J(\psi, \nabla^2 \psi) - J(\tau, \nabla^2 \tau) - \frac{1}{2} k \nabla^2 \psi + \frac{1}{2} k \nabla^2 \tau \tag{1}$$

$$\frac{\partial}{\partial t} \nabla^2 \tau = - J(\psi, \nabla^2 \tau) - J(\tau, \nabla^2 \psi) + f \nabla^2 \chi + \frac{1}{2} k \nabla^2 \psi - \frac{1}{2} k \nabla^2 \tau - K \nabla^2 \tau \tag{2}$$

$$\frac{\partial}{\partial t} \theta = -J(\psi, \theta) - J(\tau, \sigma) + \nabla \cdot (\sigma \nabla \chi) - (j + \frac{1}{2} h) (\theta - \theta^*) + \frac{1}{2} h (\sigma - \sigma^*) \tag{3}$$

$$\frac{\partial}{\partial t}\sigma = -J(\psi,\sigma) - J(\tau, \theta) + \nabla\theta \cdot \nabla\chi$$

$$+ \frac{1}{2} h (\theta - \theta^*) - (j + \frac{1}{2} h) (\sigma - \sigma^*) - H(\sigma - \sigma_c) \qquad (4)$$

$$f \nabla^2 \tau = -\frac{1}{2} c_p (p_3^\kappa - p_1^\kappa) p_o^{-\kappa} \nabla^2 \theta \qquad (5)$$

The operating symbols have their conventional meaning; the other symbols represent the following quantities:

ψ	Stream function for mean wind
τ	Stream function for mean wind shear
χ	Velocity potential for the lower layer in the two-layer model
θ	Vertical mean of potential temperature
θ^*	Vertical mean of externally imposed (radiation equilibrium) potential temperature
σ	Static stability (potential temperature differences between upper and lower layer)
σ^*	Externally imposed (radiation equilibrium) static stability parameter
f	Coriolis parameter (assumed constant)
p_o, p_1, p_3	Pressures at ground and at centers of lower and upper layer
c_p, c_v	Specific heats of air
κ	$(c_p - c_v)/ c_p$
k	Rate of momentum exchange near the ground
K	Rate of momentum exchange in the free atmosphere
h	Rate of radiational and turbulent heat exchange near the ground
j	Rate of radiational heat exchange in the free atmosphere

H Rate of convective heat exchange in the free atmosphere

σ_c Critical stability

The meaning of most terms is self-evident; in particular the Jacobians present the effect of advection and the linear terms the effect of nonadiabatic processes. Equation (5) is the thermal wind equation. The effect of convection as represented by the last term in equation (4) requires some explanation. Vertical mixing in dry air would tend to produce a uniform potential temperature; that means it would tend to drive the stability parameter σ towards zero. In the actual atmosphere the establishment of such a dry-adiabatic lapse rate is generally prevented by condensation. In the present model it has therefore been assumed that convection drives the vertical stability not towards zero but towards some larger critical value, σ_c.

6. Expansion in Series

One of us (Lorenz, 1960 a) has described the advantages, in problems of this sort, of simplifying the equations by expanding the field of each variable in a suitable set of orthogonal functions, and then omitting reference to all but a few of these functions. The choice of orthogonal functions must depend upon the region involved.

We shall deal with a region bounded by two parallel infinite walls at the latitudes where $y = 0$ and $y = v$. We shall further require that all functions be periodic in x, with the period $2v$.

Since there can be no flow of mass across the walls, the stream function, and hence, through the thermal wind relation, the temperature can be considered constant on each wall. The set of orthogonal functions

$$
\begin{aligned}
F_{nm} &= 1 && \text{for } n = 0 \quad m = 0 \\
&= \sqrt{2} \cos my/a && \text{" } n = 0 \quad m > 0 \\
&= 2 \sin my/a \cos nx/a && \text{" } n > 0 \quad m > 0 \\
F'_{nm} &= 2 \sin my/a \sin nx/a && \text{" } n > 0 \quad m > 0
\end{aligned}
\tag{6}
$$

where $a = w/\pi$, is therefore suitable. The expansions for ψ, τ, $\nabla^2 \chi$ and θ in these orthogonal functions are then truncated by retaining only those functions for which $m \leq 2$ and $n \leq 4$. In the expansion for σ, only the function F_{oo} is retained, so that static stability is regarded as a function of time alone. Details of the expansions appear in the appendix.

These expansions are then substituted into the governing equations (1) - (5). The products of orthogonal functions, which appear on the right, may themselves be expanded in series of orthogonal functions, which must be similarly truncated. There results a set of 56 ordinary differential equations in which the 56 dependent variables are the coefficients in the expansions for ψ, τ, $\nabla^2 \chi$, θ and σ.

These equations have been further simplified by omitting the interactions between different wave numbers (products of two orthogonal functions with two different non-zero values of n), while the interaction of each wave with the zonal current is retained. The complete

set of equations appears in the appendix.

7. Scales and Numerical Values of Coefficients

The area between the two latitudinal boundary walls is supposed to be bisected by the 30th parallel. The length of this parallel around the globe is about 34 800 km. We assume a cyclical repetition of the motion pattern every 120° of longitude; that means the largest waves could occur three times around the globe and their lengths along the 30th parallel would therefore be equal to 11 600 km. This length was stipulated above to be twice the distance between the latitudinal walls; therefore $w = 5800$ km. A scale length is now defined conveniently by:

$$a = w/\pi = 1846 \text{ km} \tag{7}$$

For our time scale we set the reciprocal value of the Coriolis parameter at 30° lat. as unity.

$$f(30^{\circ}) = 7.29 \times 10^{-5} \text{ sec}^{-1} = (3.81 \text{ hours})^{-1} \tag{8}$$

One unit of time was also chosen for the time increment in the numerical integrations.

The choice of a non-dimensional unit of temperature is based on consideration of equation (5). Assuming

$$p_o/p_1/p_3 = 1000/750/250$$

we set:

$$B = \frac{2a^2 f^2 p_o^{\kappa}}{c_p(p_I^{\kappa} - p_3^{\kappa})} = 146^{\circ}\text{C} \tag{9}$$

The various rates of turbulent mixing and radiational heating have all the dimensions of inverse time and can therefore be expressed readily as multiples of f.

On the basis of the earlier computation by Bryan and by Lorenz we set arbitrarily:

Constant	Dimensionless Value
f	1
k	4/32
K	1/32
j	4/32
h	4/32
H	1/32

The critical stability $\sigma_c = 10^{\circ}C$ or 0.0685 in non-dimensional units.

8. The External Heating Function

We stipulate a variation of θ^* with cos y/a. The difference between the extreme polar and equatorial values of θ^* is assumed $75^{\circ}C$.

In addition to the resulting meridional heating gradient, we stipulate latitudinal heating differences caused by an idealized system of oceans and continents. The continents are supposed to be half as wide as the oceans between them at all latitudes. This gives them a uniform zonal extent of 40° or 3930 km - about the width of Australia or North America along the 30th parallel.

The radiation equilibrium temperature θ^* over the continents is assumed 25° higher than that over water along the 30th parallel, that means we deal with summer only in the present study. The heating difference is supposed to be zero at the polar and equatorial walls.

The variations of θ^* have been expanded on this basis with the aid of the orthogonal functions (6) into a series, which was truncated in the same way as the series for the dependent variables:

$$\theta^* = B\,(F_{nm} \cdot \theta^*_{nm})$$

The usual convention requiring summation over all products that contain the same values of m and n in both factors has been used in writing the expression (10). In the present case m is allowed to assume only the values 0 and 1, while n varies again from 0 to 4. The individual terms of the expansion have the numerical values:

$$\theta^*_{01} = 0.1815$$

$$\theta^*_{11} = 0.0460$$

$$\theta^*_{21} = 0.0230$$

$$\theta^*_{31} = 0$$

$$\theta^*_{41} = -0.0115$$

The term θ^*_{00} is an arbitrary constant and the coefficient B has been defined by the relation (9).

The vertical heating rate as determined by σ^* is a constant parameter of the computation. It is the basic aim of this paper to study the various circulation patterns which are associated with different values of this parameter σ^*.

9. Discussion of Computation Results

The numerical computations were performed on a Royal-McBee

LGP-30 electronic computer. Starting from arbitrary initial conditions, we permitted the computer to operate until a statistically stationary state had apparently been reached. Means and variances of the coefficients in the expansions of ψ , θ and σ were then formed from the subsequent computations. In most cases these were based on a sample, made up by every fourth time step in a computational run covering 800 steps, or approximately four and a half months.

Radiational cooling in the free atmosphere should tend to increase baroclinic and convective instability. The effect is measured by σ^*. In the present series of computations we used the values $\sigma^* = -5^o$, 0^o and 5^o for this parameter.

From the statistical means of the dependent variables, it was possible to construct mean "climatological" maps of the model. These maps, as reproduced in figures 2, 3 and 4 show several features which the observational analysis had lead us to expect. The most stable case, that is the case of least cooling at high levels, $\sigma^* = 5^oC$, is associated with the fastest thermal wind, a more zonal pattern, an eastward shift of quasi-stationary features and a much weaker "climatological" high pressure cell over the oceans. The differences between the cases $\sigma^* = 0$ and $\sigma^* = -5$ are less pronounced.

The mean maps tell only part of the story. Plotting of a series of instantaneous model maps shows individual pressure centers of about equal intensity in all three cases. However, in the case $\sigma^* = 5^o$, these large cyclones and anticyclones move with an average

speed of about 7 or 8 degrees of long. per day. With the higher rates of upper cooling, characterized by $\sigma^* = 0^o$ or $\sigma^* = 5^o$ the speed of translation is much more irregular and averages only about 5 degrees long. per day.

An even greater difference is associated with the longevity of the travelling pressure centers. In the case $\sigma^* = 5^o$ their intensity changes little over long periods of time. In the more stable cases, there is a strong tendency for anticyclogenesis over the western tropical oceans and for cyclogenesis over the western parts of the continents at higher latitudes. The appearance of the climatological highs and lows in the maps for the cases $\sigma^* = 0$ and $\sigma^* = -5^o$ are due to these developments. The climatological pressure centers are most pronounced for $\sigma^* = 0$. In the case $\sigma^* = -5$, the picture becomes somewhat blurred by the emergence of smaller disturbances with higher wave numbers.

The deduction is confirmed by a study of table 3, which lists the mean integrated kinetic energies associated with the different wave numbers n for different values of σ^*. Disturbances characterized by $n = 2$ or $n = 3$ are mainly responsible for the appearance of pressure centers in the "climatological" maps. It can be seen from the table that the energy associated with these waves is as large in the case $\sigma^* = 5^o$ as in the two other ones, but because of their small intensity variation and rapid translation this does not appear in the mean climatological picture.

Table 3. Mean Kinetic Energies per Unit Mass ($m^2 sec^{-2}$) Associated with Different Wave Numbers n for Different Values of σ^*

n	-5^oC	0^o	5^o
0	9.1	20.3	47.4
1	13.4	15.2	15.9
2	22.2	54.2	81.6
3	151.3	105.1	93.9
4	51.1	1.5	1.0
Total	247.1	195.3	238.8

There is surprisingly little variation between the values of the total kinetic energy in the three cases. The energy of the zonal motion (n = 0) and the very long waves (n = 1,2) increases with increasing stability; that of the shorter waves (n = 3,4) decreases. In fact, wave number 4 probably would not appear at all in the more stable cases without a forcing function. The minimum of the total kinetic energy which characterizes the case $\sigma^* = 0^o$ may be explicable by the contrary variation of the longer and shorter waves with vertical stability.

The rate of convective heat transport through the free atmosphere, in our model, is proportional to $(\sigma_c - \sigma_o)$. The concept of convection includes in this case not only phenomena on the cumulus scale, but also the effect of all waves with numbers larger than four. Table 4 lists values of the time mean of σ_o associated with different values of σ^*.

Table 4. Time Mean and Standard Deviation of σ_o Associated with Different Vertical Cooling Gradients

σ^* (°C)	-5	0	5
Time mean of σ_o	7.1	8.9	12.6
Stand. dev. of σ_o	0.8	1.3	1.1

The comparatively large difference between $\sigma^* = 0^o$ and $\sigma^* = 5^o$ as compared to that between $\sigma^* = 0^o$ and $\sigma^* = -5^o$ is again evident. With $\sigma_c = 10^o$, the sign of $(\sigma_c - \sigma_o)$ is positive for the two cases $\sigma^* = -5^o$ and $\sigma^* = 0$. Convective mixing transports heat upward in these two cases. It transports heat downwards in the other case.

10. Comparison of the Numerical Model with Actual Climatic Regimes

In establishing any relationship the great simplification involved in our model has to be considered. We neglected the convergence of the meridians and the variation of the Coriolis parameter f with latitude. We also used only two parameters, m = 1 and m = 2, to characterize the mean meridional distribution of wind and temperature. In the actual atmosphere the mean meridional motion probably involves three cells at least in winter - a tropical and a polar direct meridional circulation, and an indirect circulation in temperate latitudes. This three-cell system cannot be simulated with two values of m. The omission is permissible for the present case of summer conditions with the polar boundary of our strip at about 60^o lat. It would become important if a larger part of the

hemisphere were to be modeled during winter.

The model agrees with the deductions from natural observations in showing positive correlations between vertical stability, zonal winds at high levels, and eastward displacement of the mean position of pressure centers. It also suggests a qualitative explanation for the changes in rainfall regimes and hurricane incidence. The mean upward heat flux and convection $(\sigma_c - \sigma_o) > 0$ associated with the more unstable cases $\sigma^* = -5^o$ and $\sigma^* = 0$ might be alone sufficient to account for a wetter regime in low latitudes. The frequent anti-cyclogenesis off the subtropical east coasts in the model and the resulting surges from the east could explain the extension of this higher rainfall regime to temperate latitudes along the east coasts. The climatic mean maps associated with the more unstable values of σ are also obviously conducive to a relatively frequent northward steering of hurricanes along the east coasts. It is of interest to note that a somewhat similar mean synoptic situation was associated by Flohn (1952) with the establishment of the North American ice age.

The shorter wave lengths associated with lower stability might also be favorable to more frequent northerly winds over the oceans and therefore to a higher evaporation rate.

A decrease in the vertical gradient of the cooling rate - that is, a higher value of σ^* in our model - would be compatible with the climatic changes which occurred about the turn of the century and which were described at the beginning of this paper.

Our model fails to account for the warming at high latitudes which appears to accompany the dry periods at low latitudes, or for the colder regime which exists there during wetter periods. In fact, as can be seen from figure 4, the mean meridional temperature gradient increases with increased stability in the model.

This discrepancy may be the result of specific simplifications in the model; in particular, the lack of horizontal variability of stability, the absence of a third cell in high latitudes, and the omission of evaporation and condensation. One might argue, for example, that an increase in ozone mixing ratio would increase the stability at low latitudes while decreasing it at high latitudes because of surface heating (Plass, 1956). One could also argue that reduced evaporation in low latitudes would be conducive to a greater poleward transport of heat by ocean currents.

Further investigations along the present lines can now be readily defined. It would be of interest to introduce a seasonal variation of σ^* and to use at least three meridional wave numbers instead of two. We also might gain a better insight by a modification of the present model which would permit introduction of a horizontally variable stability σ and Coriolis parameter f. At a later stage, an attempt might be made to extend the number of layers in the model and to include in this way the circulation of the stratosphere and perhaps of the oceans separately.

Acknowledgement: Part of this study was carried on while both authors were at the National Center for Atmospheric Research. A portion of the work has been sponsored by the Geophysics Research Directorate of the Air Force Cambridge Research Center under Contract No. AF 19(604) - 4969. Many of the numerical computations were carried out by Mrs. Margaret Hamilton and Miss Ellen Fetter of M.I.T. and Miss Astrik Deirmendjian of N.C.A.R.

References

Bryan, K. 1959 A numerical integration of certain features of the general circulation, Tellus, Vol. 11, p. 163.

Flohn, H. 1952 Allgemeine Atmosphärische Zirkulation und Palaoklimatologie, Geol. Rundschau, Vol. 40, p. 153.

Kraus, E. B. 1954 Secular changes in the rainfall regime of S. E. Australia, Quart. J R Met Soc., Vol. 80, p. 591.

1958 Recent climatic changes, Nature, Vol. 181, p. 666.

1960 Synoptic and dynamic aspects of climatic change, Quart. J. R Met. Soc., Vol. 86, p. 1.

Lorenz, E. N. 1960(a) Maximum simplification of the dynamic equations, Tellus, Vol. 12, p. 243.

1960(b) Energy and numerical weather prediction, Tellus, Vol. 12, p. 364.

Plass, G. N. 1956 The influence of the 9.6m ozone band on the atmospheric infra-red cooling rate, Quart. J. R. Met. Soc., Vol. 82. p. 30.

APPENDIX

The right hand sides of the partial differential equations (1)-(4) contain quadratic functions of the dependent variables $\psi, \tau, \chi, \theta,$ and σ. When these variables are expressed as truncated series of the orthogonal functions F_{oo}, F_{om}, F_{nm}, and F'_{nm}, and the series are substituted into equations (1) - (4), the right hand sides of the resulting equations will contain Jacobians of the orthogonal functions. These Jacobians must be expressed as new truncated series of orthogonal functions.

The expansions which will concern us are as follows:

$$a^2 J(F_{o\kappa}, F_{nm}) = -\sum_{\ell=1}^{\infty} n\gamma_{\kappa\ell m} F_{n\ell}' \quad , \tag{11}$$

$$a^2 J(F_{o\kappa}, F_{nm}') = \sum_{\ell=1}^{\infty} n\gamma_{\kappa\ell m} F_{n\ell} \quad , \tag{12}$$

$$a^2 J(F_{n\ell}, F_{nm}') = -\sum_{\kappa=1}^{\infty} n\gamma_{\kappa\ell m} F_{o\kappa}$$

$$- \frac{1}{2} n(\ell - m) F_{\ell + m, 2n} + \frac{1}{2} n (\ell + m) F_{\ell - m, 2n} \tag{13}$$

$$a^2 J(F_{n\ell}, F_{nm}) = -a^2 J(F_{n\ell}', F_{nm}')$$

$$= \frac{1}{2} n(\ell - m) F'_{\ell + m, 2n} - \frac{1}{2} n(\ell + m) F_{\ell - m, 2n} \quad , \tag{14}$$

where

$$\gamma_{\kappa\ell m} = \frac{2\sqrt{2}}{\pi} \int_0^\pi \kappa \sin \kappa\gamma \sin \ell\gamma \sin m\gamma \, d\gamma \qquad (15)$$

$$= 0 \text{ if } \kappa + \ell + m \text{ is even}$$

$$= \frac{\sqrt{2}}{\pi} \kappa \left(\frac{1}{\kappa + \ell - m} + \frac{1}{\kappa - \ell + m} + \frac{1}{-\kappa + \ell + m} - \frac{1}{\kappa + \ell + m} \right)$$

if $\kappa + \ell + m$ is odd.

We now introduce the index s, and, for values of s from 1 through 6, define the orthogonal functions $G_s(n)$ according to table 5. The corresponding eigenvalues $C_s(n)$, which satisfy the relation $a^2 \nabla^2 G_s = -C_s G_s$, also appear in table 5.

Table 5. Values of $G_s(n)$ and $C_s(n)$

S	1	2	3	4	5	6
$G_s(n)$	F_{01}	F_{n1}	F'_{n1}	F_{02}	F_{n2}	F_{n2}'
$C_s(n)$	1	$n^2 + 1$	$n^2 + 1$	4	$n^2 + 4$	$n^2 + 4$

For simplicity we first consider the case where the series of orthogonal functions are further truncated so that only one non-zero value of n occurs, i.e., the total circulation consists of a zonal circulation plus disturbances of a single wave length. We may then write the truncated expansions for the dependent variables as:

$$\psi = a^2 f \sum_s \psi_s G_s \quad , \tag{16}$$

$$\tau = a^2 f \sum_s \tau_s G_s \quad , \tag{17}$$

$$\nabla^2 \chi = f \sum_s \omega_s G_s \quad , \tag{18}$$

$$\theta = B(\theta_0 + \sum_s \theta_s G_s) \quad , \tag{19}$$

$$\sigma = B \sigma_0 \quad . \tag{20}$$

The constants in (16) - (20) make the new variables dimensionless. The thermal wind equation (5) tells us that $\tau_s = \theta_s$. To express the new differential equations in a concise form, we introduce a second index r(s), related to s according to table 6. We also introduce coefficients α_s.

Table 6. Values of r(s) and α_s

s	1	2	3	4	5	6	7	8	9	10	11	12	13
r(s)	2	3	1	2	6	1	5	6	4	5	3	4	2
α_s	γ_{111}	γ_{111}	γ_{111}	γ_{212}	γ_{122}	γ_{122}	γ_{122}	γ_{212}	γ_{212}	γ_{212}	γ_{212}	γ_{212}	γ_{212}

We shall adopt the convention that $\bar{G}_s = G_{r(s)}$, $\bar{C}_s = C_{r(s)}$, etc. With this convention, we may write the truncated form of equations (11) - (13) as

$$a^2 J(\bar{G}_s, \bar{G}_{s+1}) = \begin{cases} -n\alpha_s G_s & , s = 1, \ldots, 6 \\ -n\alpha_s G_{s-6} & , s = 7, \ldots, 12. \end{cases} \tag{21}$$

When the truncated series (16) - (20) are substituted into the governing equations (1) - (4), the resulting equations may now be written in the form

$$\dot{\psi}_s = nC_s^{-1}(\bar{C}_{s+1} - \bar{C}_s)\alpha_s(\bar{\psi}_s\bar{\psi}_{s+1} + \bar{\theta}_s\bar{\theta}_{s+1}) + nC_s^{-1}(\bar{C}_{s+7} - \bar{C}_{s+6})\alpha_{s+6}(\bar{\psi}_{s+6}\bar{\psi}_{s+7} + \bar{\theta}_{s+6}\bar{\theta}_{s+7}) - \frac{1}{2}\kappa(\psi_s - \theta_s) \tag{22}$$

$$\dot{\theta}_s = nC_s^{-1}(\bar{C}_{s+1} - \bar{C}_s)\alpha_s(\bar{\psi}_s\bar{\theta}_{s+1} + \bar{\theta}_s\bar{\psi}_{s+1}) + nC_s^{-1}(\bar{C}_{s+7} - \bar{C}_{s+6})\alpha_{s+6}(\bar{\psi}_{s+6}\bar{\theta}_{s+7} + \bar{\theta}_{s+6}\bar{\psi}_{s+7}) - C_s^{-1}\omega_s + \frac{1}{2}\kappa\psi_s - (\frac{1}{2}\kappa)\theta_s \tag{23}$$

$$\dot{\theta}_0 = -(j + \tfrac{1}{2}h)(\theta_0 - \theta_0^*) + \tfrac{1}{2}h(\alpha_0 - \alpha^*) \tag{24}$$

$$\dot{\theta}_s = n\alpha_s(\bar{\psi}_s\bar{\theta}_{s+1} - \bar{\theta}_s\bar{\psi}_{s+1}) + n\alpha_{s+6}(\bar{\psi}_{s+6}\bar{\theta}_{s+7} - \bar{\theta}_{s+6}\bar{\psi}_{s+7}) + \sigma_0\omega_s - (j + \tfrac{1}{2}h)(\theta_s - \theta_s^*) \tag{25}$$

$$\dot{\sigma}_0 = -\sum_s \theta_s\omega_s + \tfrac{1}{2}h(\theta_o - \theta_0^*) - (j + \tfrac{1}{2}h)(\sigma_0 - \sigma^*) - H(\sigma_0 - \sigma_c) \tag{26}$$

Here a dot denotes a derivative with respect to "dimensionless time" ft. It is possible to eliminate ω_s from the alternative expressions (23) and (25) for $\dot{\theta}_s$ and also from equation (26).

We now consider the more general case where several non-zero values of n are permitted. In the present study these values are n = 1, 2, 3,4. The truncated series for ψ now takes the form

$$\psi = \sum_s \left(\sum_n \psi_s(n) \; G_s(n) \right.$$

with analogous expansions for τ, $\nabla^2 \chi$, and θ, where it is understood that the summation over n runs from 1 to 4 if s = 2,3,5 or 6, but that only the value n = 0 occurs if s = 1 or 4.

If interactions between different wave numbers are suppressed, while the interaction of each wave number with the zonal current is retained, the governing differential equations will be unaltered, except that in certain terms summations over n will appear. Specifically, in equations (22), (23), and (25), when the index s on the left hand side has the value 1 or 4, the quadratic terms on the right hand side are summed over n, but otherwise there is no summation over n, and each equation stands for four equations, one for each value of n. Equation (24) is unaltered, while the quadratic term in equation (26) is to be summed over n and s.

Legend of Figures

1. Cumulative percentual deviations from the 1881-1940 annual mean. (1) N. W. New South Wales (Australian rainfall district No. 48); (2) Queensland Coast (Australian rainfall district No. 40); (3) Carolina Coast (mean of Charleston and Cape Hatteras); (4) India (peninsula); (5) Nile discharge at Aswan; (6) Central Cape Province (South Africa rainfall district No. 16A).

2. Contour lines ($\Psi - \tau$) for lower layer.

3. Contour lines (Ψ) for mean flow.

4. Lines of equal mean potential temperature Θ.

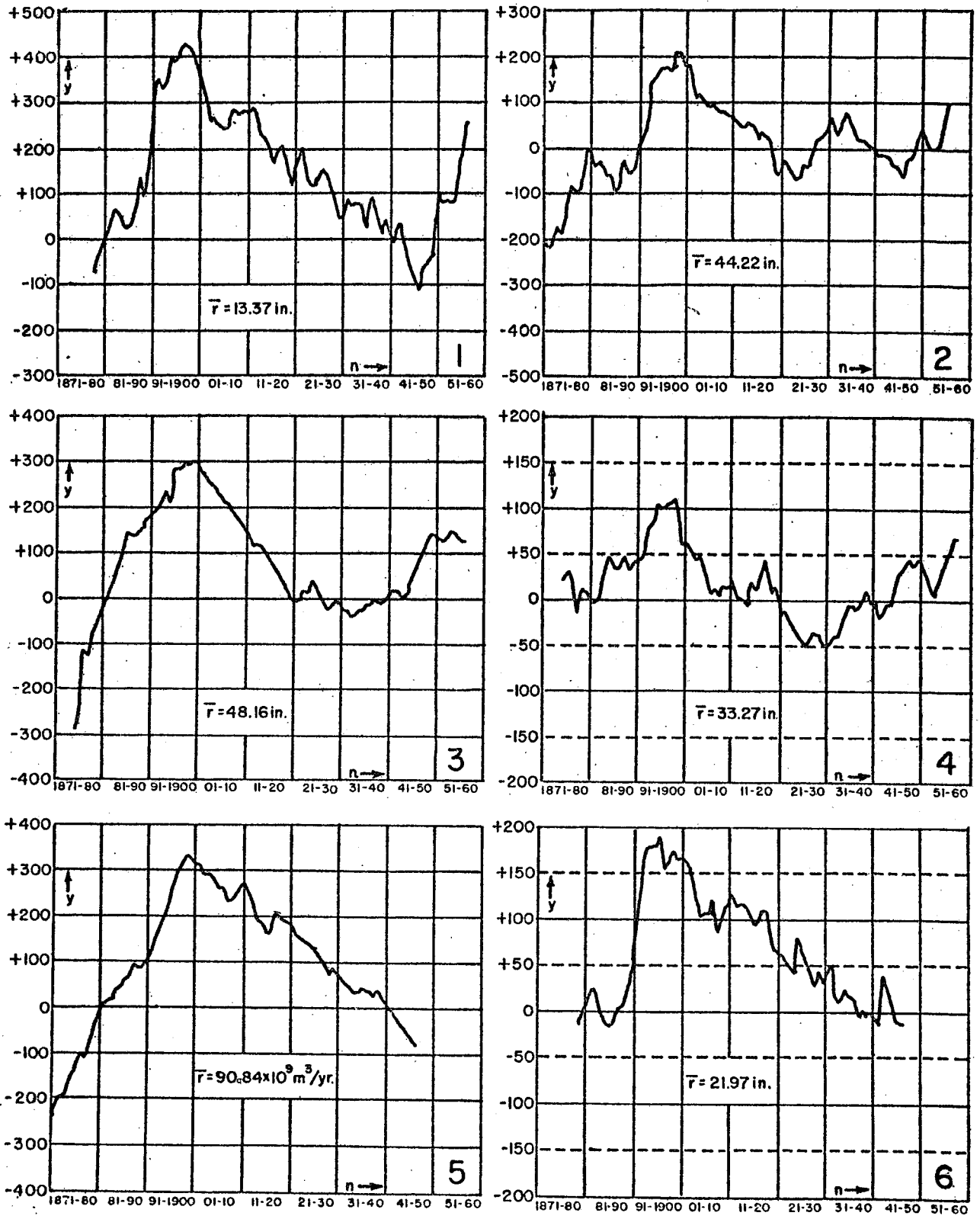
+500
+400
+300
+200
+100
0
-100
-200
-300
y
$\bar{r}$ = 13.37 in.
n →
1
1871-80 81-90 91-1900 01-10 11-20 21-30 31-40 41-50 51-60
+300
+200
+100
0
-100
-200
-300
-400
-500
y
$\bar{r}$ = 44.22 in.
n →
2
1871-80 81-90 91-1900 01-10 11-20 21-30 31-40 41-50 51-60
+400
+300
+200
+100
0
-100
-200
-300
-400
y
$\bar{r}$ = 48.16 in.
n →
3
1871-80 81-90 91-1900 01-10 11-20 21-30 31-40 41-50 51-60
+200
+150
+100
+50
0
-50
-100
-150
-200
y
$\bar{r}$ = 33.27 in.
n →
4
1871-80 81-90 91-1900 01-10 11-20 21-30 31-40 41-50 51-60
+400
+300
+200
+100
0
-100
-200
-300
-400
y
$\bar{r}$ = 90.84 x 10^9 m^3/yr.
n →
5
1871-80 81-90 91-1900 01-10 11-20 21-30 31-40 41-50 51-60
+200
+150
+100
+50
0
-50
-100
-150
-200
y
$\bar{r}$ = 21.97 in.
n →
6
1871-80 81-90 91-1900 01-10 11-20 21-30 31-40 41-50 51-60

Figure 1

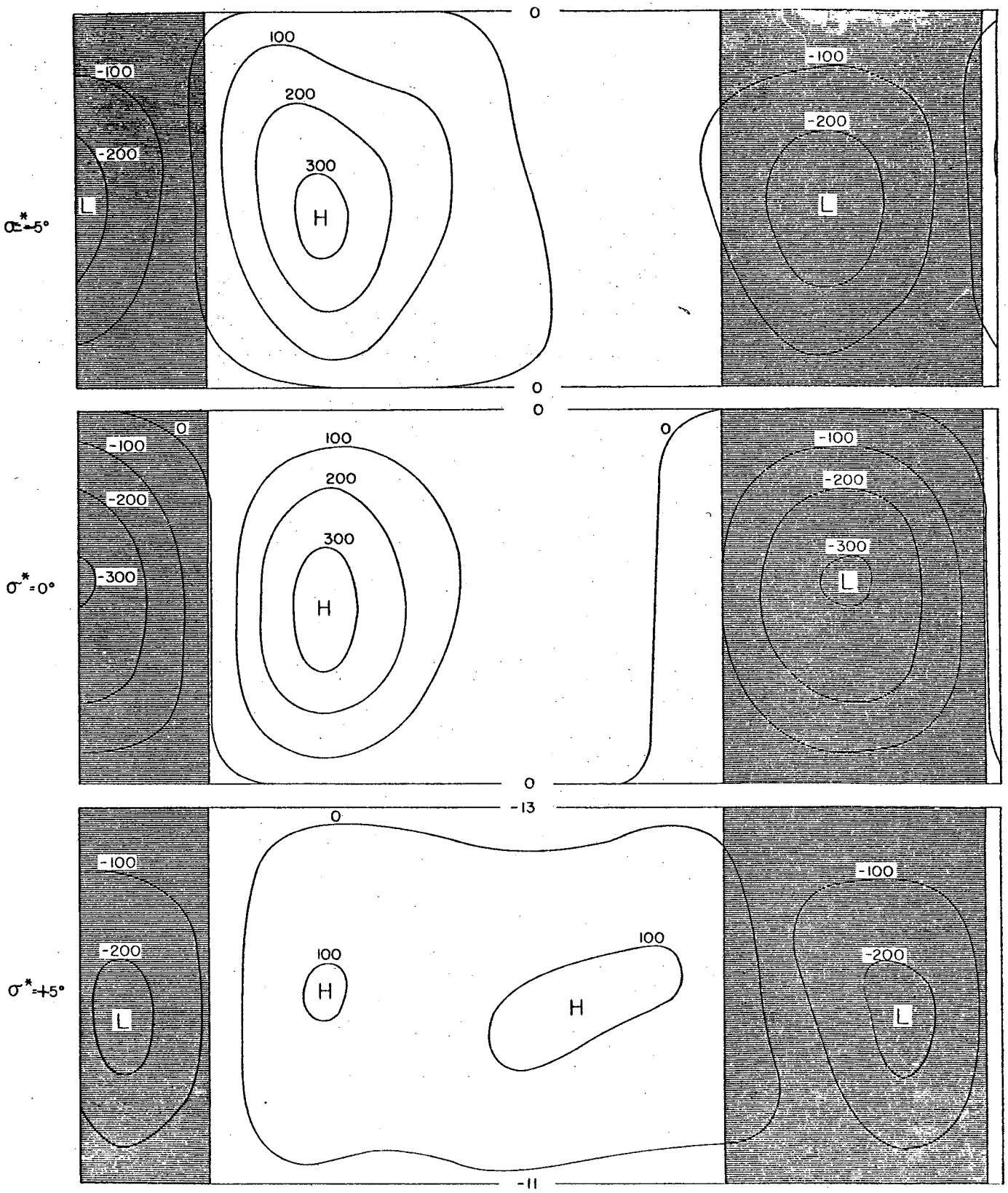
α*=-5°
0
100
200
300
H
-100
-200
L
0
-100
-200
L
0
0
100
200
300
H
-100
-200
-300
L
0
0
-13
σ*=+5°
0
100
H
100
H
-100
-200
L
-100
-200
L
-11

Figure 2

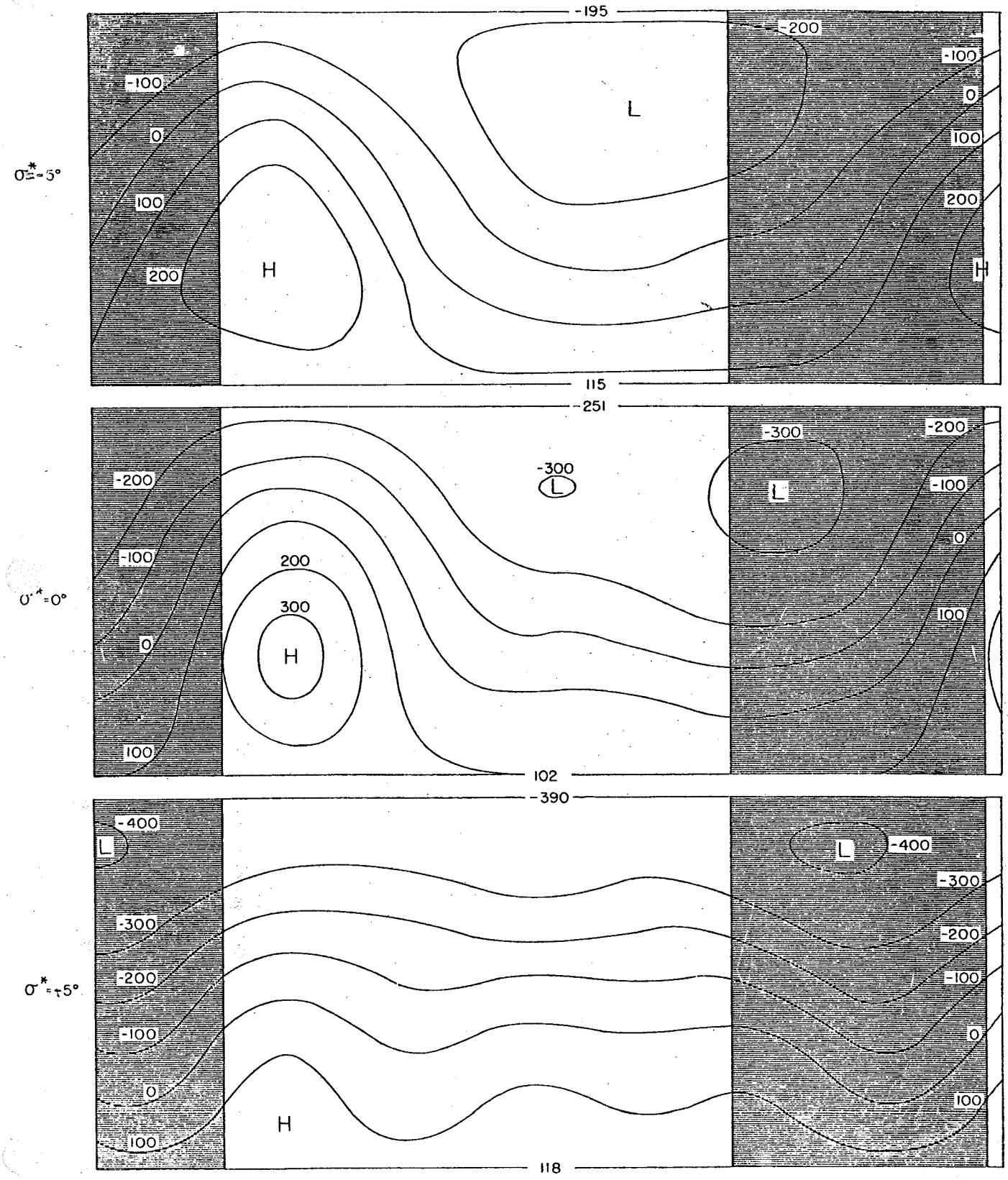
$\sigma^*_{\Xi}=5°$
-195
-200
-100
0
100
200
L
H
H
115
-251
-300
-200
-100
0
100
200
300
L
L
H
102
$\sigma^*=0°$
-390
-400
-300
-200
-100
0
100
L
L
H
118
$\sigma^*_{=}+5°$

Figure 3

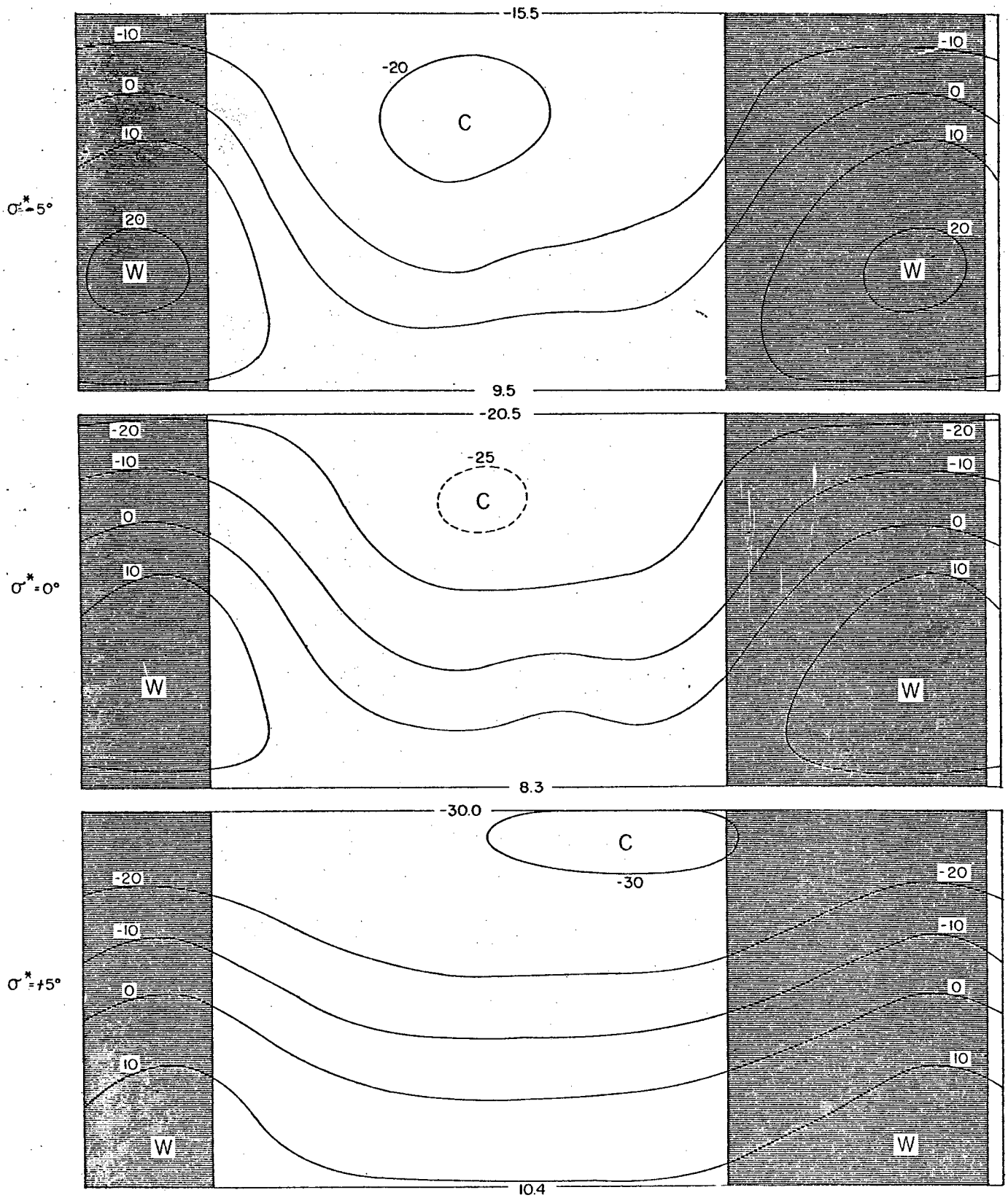
-15.5
-10
0
10
20
-20
C
W
9.5
$\sigma^* = 5°$
-20.5
-20
-10
0
10
-25
C
W
8.3
$\sigma^* = 0°$
-30.0
C
-30
-20
-10
0
10
W
10.4
$\sigma^* = +5°$

Figure 4